JOURNAL OF MATERIALS SCIENCE 3 (1968) 577–583

Preprecipitation in Al/Zn/Mg Alloys Studied by Hardness and Small-Angle X-ray Scattering Measurements

P. BARDHAN, E. A. STARKE JR
School of Chemical Engineering, Georgia Institute of Technology, Atlanta, Georgia, USA

Received 25 March 1968, and in revised form 26 April

Small-angle X-ray scattering techniques and hardness measurements have been used to study preprecipitation in two Al/Zn/Mg alloys containing the same Zn content (2.46 at. %) but different Mg contents. Changes in Guinier-Preston (G-P) zone size are observed to follow the same pattern as changes in hardness. It is also observed that a critical zone size is required for the nucleation of the intermediate precipitate, η'; the size being dependent on the Mg content. The role of Mg as a reversible-vacancy trap is also established.

1. Introduction

Preprecipitation in Al/Zn/Mg alloys has received a great deal of attention in recent years. Several studies have been made of the variation of mechanical properties during ageing, principally by Polmear [1-3]. As a result of these studies, Polmear [2] constructed a surface in the phase diagram of the ternary alloy to represent the upper temperature limit for Guinier-Preston zone stability. This surface was later modified somewhat by Lorimer and Nicholson [4]. Besides extensive electron microscopy studies to determine the distribution and morphology of the preprecipitates and precipitates [4-9], a variety of other techniques, including electrical resistivity [10-13] and small-angle X-ray scattering [14-18], have been used to characterise the structural changes during the decomposition of the ternary alloys.

Early work by Nicholson, Thomas, and Nutting [5] revealed a completely homogeneous type of preprecipitation. The initial stages of ageing could not be studied, however, as the first clusters formed are smaller than the lower limit of resolution of the electron microscope. Thus the G-P zones could be observed only after they had reached a certain size, generally about 10 Å. The later stages showed the existence of a partially coherent precipitate, which from their electron diffraction patterns was found to lie on the {1 1 1} planes of the matrix, confirming the X-ray results of Mondolfo *et al* [19]. It was also observed that the intermediate precipitate was formed by transformation of the coherent zones to the partially incoherent structure which characterises the η' phase. It appeared that the smaller zones remained untransformed around the precipitate, then dissolved in the matrix. Thereafter, it was suggested that a dispersion-hardening mechanism operated in these alloys. The alloys were found to soften with the formation of coarse incoherent precipitates. In later studies, Nicholson, Thomas, and Nutting [6] found little evidence of any preferential nucleation of the intermediate precipitate along single dislocations. From this and from a study of the effect of subgrain structure, Holl [20] concluded that the controlling factor for the nucleation of the intermediate precipitate was probably not the vacancy concentration (trapped during the quench from the high temperature) but a critical zone size. Embury and Nicholson [7] maintained, however, that the apparently homogeneous nucleation of precipitates within the grains was largely governed by the concentration and distribution of vacant lattice sites.

From a review of the literature, it is evident that the process of preprecipitation in the Al/Zn/Mg alloy system is quite complex and has not been completely explained. The aged

structure and the kinetics of ageing depend on both the Zn and Mg concentration and the temperatures of solution and ageing treatments. For the present study it seemed worthwhile to investigate the ageing sequence of two alloys of the same Zn, but different Mg, concentration, so that the dependence of the structure on the Mg composition, and its consequent effect on hardening, could be established.

2. Experimental Methods

The two alloys examined in this study had the following compositions as determined from chemical analysis.

Alloy 1: Al/2.46 at. % Zn/0.72 at. % Mg
Alloy 2: Al/2.47 at. % Zn/1.09 at. % Mg

They were prepared by melting high purity (99.999 %) Al, Zn, and Mg in a graphite crucible, using an electric resistance furnace. The as-cast ingots were homogenised for 2 weeks at 200° C and 1 week at 500° C. Samples were cut from the homogenised ingots and rolled to convenient thicknesses for hardness and X-ray studies. These specimens were solution-treated for 2 h at 460° C, ice-brine quenched, and immediately placed in the ageing bath. The ageing temperature chosen was 135° C, which is well below the metastable phase boundary determined by Polmear [2] and modified by Lorimer and Nicholson [4] for alloys of this composition. The ageing kinetics for both alloys are sufficiently rapid at this temperature to achieve peak hardness in a reasonable length of time. The alloys were aged for various times in the silicone oil bath at 135 $\pm$ 1° C and ice-water quenched. Hardness measurements and X-ray examinations were conducted immediately following the ageing treatments.

Hardness measurements were made with a Vickers pyramid diamond indenter using 5 and 10 kg loads. The samples, which were 2.5 $\times$ 1.3 $\times$ 0.25 cm, were large enough to allow all impressions to be made on the same specimen; however, duplicate samples were also used for reproducibility checks.

The small-angle X-ray examinations were carried out on foils approximately 0.07 mm thick, which is $\sim 1/\mu$m for the alloys under study, at 82° K, using a Kratky camera equipped with a low-temperature attachment. The unit was automated with a step-scanner and print-out and employed Ni-filtered Cu radiation. The sample-to-detector distance was 20 cm. Two sets of slits were used during the study. For short ageing times a 101 μm entrance slit and a 400 μm exit slit were used, after which a 60 μm entrance slit and a 200 μm exit slit were used. All data were corrected for background over the complete scattering range and converted to relative absolute intensity units following the method of Kratky *et al* [21]. The "infinite beam" approximation was used, as the intensity along the line shaped beam was constant for a distance of 30 mm.

High-angle X-ray measurements were made using a Nonius Guinier-de-Wolff quadruple focusing camera, and a General Electric XRD-6 diffractometer equipped with a step-scanner and Warren doubly-bent monochromator described elsewhere [22].

3. Experimental Results

The ageing sequence in two ternary Al/Zn/Mg alloys has been studied in terms of their structure and strength. The choice of two compositions, Al/2.47 at. % (5.82 wt %) Zn/1.09 at. % (0.71 wt %) Mg, and Al/2.46 at. % (5.77 wt %) Zn/0.71 at. % (0.51 wt %) Mg, permitted a study of the affect of the Mg content on the ageing phenomenon in these alloys. Hardness measurements provided an indication of the strength, as well as the progress of ageing, and was thus used to select the ageing times for X-ray investigation. Powder diffraction methods and diffuse X-ray investigations were undertaken to obtain detailed information on the nature of the structure responsible for the hardening, while small-angle scattering studies were used for quantitative analysis of the size and volume-fraction of the G-P zones at various stages of ageing.

Fig. 1 shows the hardness versus log ageing time curves at 135° C for both alloys. The lower Mg alloy has an as-quenched hardness of 30 VPN which increases linearly with ageing up to 48 VPN in about 6 h. This is followed by a period of accelerated hardening which lasts for about 5 h. The hardness then levels out until about 35 h of ageing, after which the hardness increases rapidly again to a peak hardness of 70 VPN. Overageing is seen to result after 110 h. The higher Mg content alloy also exhibits a two-stage hardening sequence. A linear increase in hardness from 40 to 86 VPN occurs in the first $2\frac{1}{2}$ h, followed by a period of constant hardness. Rapid hardening occurs immediately thereafter at a diminishing rate until a peak

hardness of 120 VPN is attained after 60 h of ageing.

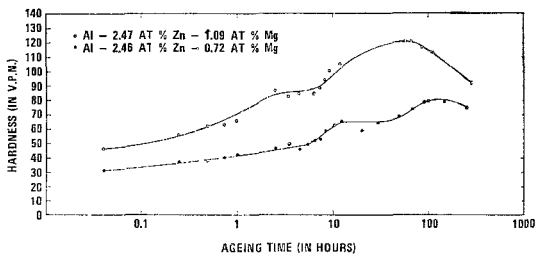

Figure 1 Hardness in VPN versus log ageing time in hours for samples aged at 135° C in silicone oil baths.

The results of the small-angle scattering experiments on the Mg-poor alloy are shown in fig. 2, which are plots of the relative absolute diffracted intensity versus s, where s is ϵ/λ and ϵ is the diffraction angle in radians and λ the wavelength of the X-rays in Å. The scattering from the alloy, after the solution-heat-treatment, in the as-quenched condition, is seen to be negligible. The small-angle scattered intensity is found to increase with progressive ageing, and appears to become concentrated in a narrow region about the primary beam. The results of similar measurements on the Mg-rich alloy are given in fig. 3. Fig. 4 shows the variation of the integrated intensity, Q_0, with time, at 135° C for both alloys. The calculated values of the Guinier radius and the integrated intensity are given in table I. Here

$$Q_0 = K \int_0^\infty s\, E(s)\, \mathrm{d}s$$

where K is the attenuation factor of the sample [21], $s = 2 \sin \theta/\lambda$, and $E(s)$ is the corrected intensity for line collimation. A steady increase of the integrated intensity occurs in the initial stages but in the later stages the intensity increases rapidly. This later anomalous increase takes place when the intermediate precipitate is thought to appear and hence is attributed to particle size effects of this phase.

The radii of the "spherical" zones were determined, at various stages of ageing, using the Guinier approximation [23] of the scattered intensity, utilising the slope of a log of scattered intensity versus ϵ^2 plot. The variation of the zone radius upon ageing at 135° C for the two alloys is shown in fig. 5.

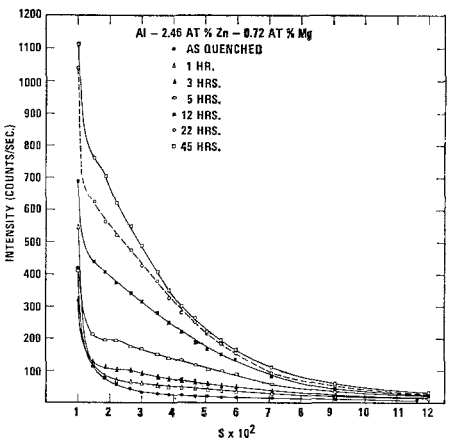

Figure 2 Corrected scattering curves for the Mg-poor alloy aged for various times at 135° C.

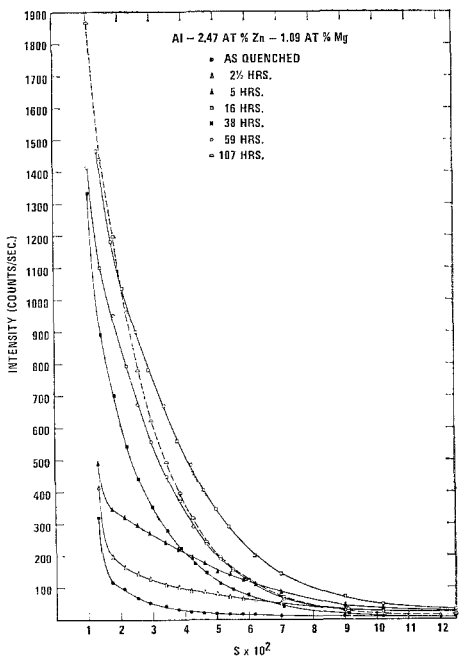

Figure 3 Corrected scattering curves for the Mg-rich alloy aged for various times at 135° C.

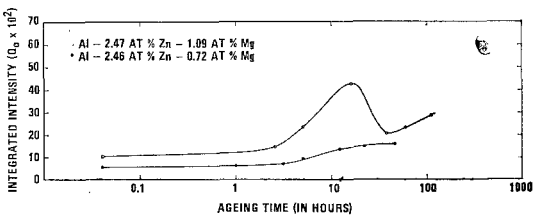

Figure 4 Integrated intensity versus log ageing time in hours for samples aged at 135° C in silicone oil baths.

TABLE I

Ageing time (h)	Al/2.46% Zn/0.72% Mg $Q_0 = K\int_0^\infty E(s)\,ds$	R_G (Å)	Al/2.47% Zn/1.09% Mg $Q_0 = K\int_0^\infty s\,E(s)\,ds$	R_G (Å)
0	0.059	13.5	0.104	13.9
1	0.063	18.0		
2.5			0.149	30.8
3	0.069	25.2		
5	0.097	30.3	0.235	35.2
12	0.134	42.1		
16			0.433	45.5
22	0.151	43.3		
38			0.205	49.6
45	0.160	45.5		
59			0.232	53.5
107			0.287	58.7

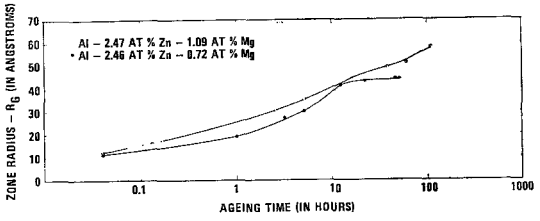

Figure 5 Zone-radius in angstroms versus log ageing time in hours for samples aged at 135° C in silicone oil baths.

4. Discussion of Results

The integrated intensity, Q_0, calculated from the scattering curve, indicates a higher value for the 1.09% Mg alloy than for the 0.72% Mg alloy. Also, it is seen that a large as-quenched hardness difference exists which cannot be completely accounted for by the solid-solution strengthening effect of Mg. High-angle X-ray diffraction was employed to analyse this difference. Extremely diffuse bands occurred in the Mg-rich alloy whose maximums corresponded to the diffraction lines of $MgZn_2$. These bands were not detected when the Mg-poor alloy was examined under similar conditions. Thus, the large difference in the hardness of the two alloys in the as-quenched state is explained as being due to the following effects.

(i) Solid-solution strengthening which accounts for only 5 to 6% of the observed 25% increase in hardness as the Mg content is raised from 0.72 to 1.09 at. % [24].

(ii) Quench clustering, whereby $MgZn_2$ clusters form during the quench in the higher Mg content alloy. Thus the higher integrated intensity in the Mg-rich alloy shows that a larger volume-fraction of the quenched-in clusters is formed in this alloy, resulting in greater hardening in this case. This phenomenon of quench-clustering also demonstrates the strong effect of small additions of Mg on the initial clustering process.

The hardness curve for the Mg-rich alloy shows a two-stage hardening when aged at 135°C, with a linear initial stage. This fact, along with the observation of $MgZn_2$ in the as-quenched state, suggests that a very small nucleation barrier exists for the formation of the G-P zones in this alloy. The $MgZn_2$ clusters occurring in the as-quenched state are present as random clusters of vacancies, Mg, and Zn. These clusters grow and progressively form the ordered GP zones observed by Gerold and co-workers [25, 26]. There is a rapid growth of these zones from about 14 Å radius to 30 Å radius, resulting in the rapid hardness increase. The first stage is followed by a period of almost constant hardness. The zone radius increases only slightly during this period until a radius of about 35 Å is reached, at which time the second stage is initiated. It appears that a critical zone size exists before these zones can act as nuclei for the formation of the η' intermediate precipitate since this precipitate accounts for the hardening in the second stage.

The appearance of the precipitate structure with resultant hardening suggests that the operative strengthening mechanism here is of a dispersion-hardening type. Maximum hardening is then a result of the combination of size and spacing between the precipitates. Softening, or overageing, finally results due to coarsening of the widely spaced precipitates.

The hardness curve of the Mg-poor alloy is more complex. Linear hardening is also observed in this case, but the rate of hardening is slower than in the Mg-rich alloy. A simple reason for this is that with less Mg there are fewer Mg-vacancy associates to aid the preprecipitation process. At a zone radius of approximately 25 Å, the hardness increases more rapidly until a zone radius of about 40 Å is reached, and then the hardness increase is arrested. It is observed that after this time the zone radius remains essentially constant. The latter is an indication of the critical size required for the nucleation of the η' intermediate precipitate. With further

growth of the η' precipitate, the second stage in the hardening curve results. No X-ray studies were made to determine the changes in precipitate size once it was formed in this alloy.

Since the increase in zone radius follows closely the changes that occur in the hardness curve, it appears that a strong correlation exists between the size of the zone and the strength of the alloy. However, it must be remembered that a distribution of zone sizes always exists, as is evident from the concave nature of the Guinier plot [23]. The sudden acceleration in the hardening rate in the first stage is accompanied by a similar rapid increase in zone radius. The difference in time associated with the accelerated hardness increase and the accelerated zone growth is attributed to the difference in quenching rates of the large hardness sample and the small X-ray sample.

The acceleration in the ageing process is explained by using the model proposed by Perry [27]. According to Perry's theory, Mg plays the role of a reversible vacancy trap. Since the Mg-vacancy binding energy is extremely high compared to the Zn-vacancy binding energy in the ternary (0.17 eV as compared to 0.05 eV) most of the vacancies associated with the solute-atoms, immediately after the quench, are attached to the Mg-atoms. The vacancy-concentration in the matrix falls with the annihilation of the free excess vacancies at sinks, such as grain-boundaries and dislocations. To maintain a more homogeneous distribution of vacancies in the alloy, Mg-atoms in the zones release the vacancies previously trapped during the quench. Thus, initially, solute clusters form with the aid of isolated vacancies being trapped by Mg-atoms. After ageing has progressed for some time, the Mg becomes activated as a vacancy source. This stage marks the accelerated ageing period prior to the incubation period for the intermediate precipitate. This model, however, must be reconciled in some way with the fact that after the increased rate of zone growth just mentioned, further growth is suddenly arrested during the time required for nucleation of the precipitate structure.

A further observation, during the nucleation of the intermediate precipitate, is that the integrated intensity is fairly constant, thus no redistribution of the solute atoms affects the nucleation and zone growth. The incubation time in this case then represents the time required to transform a fully coherent zone to a semi-coherent precipitate with a unique structure of its own. The constant zone size thus indicates that this transformation occurs only when the G-P zones have acquired a certain critical size. This observation of a critical zone size for the nucleation of the η' precipitate is consistent with the conclusion reached by Holl [20]. It does not mean, however, that all the zones have ceased to grow. The zone size obtained from the small-angle scattering data is the Guinier radius. This radius is known to be weighted in favour of the larger zones that occur in the alloy [28], since the X-ray size parameters become ratios of moments when a size distribution of particles exist. For the Kratky camera, using a line-shaped beam, the exact form for the Guinier radius was derived by Baur and Gerold [28] to be:

$$R_G = \left[\frac{<r^7>}{<r^5>}\right]^{\frac{1}{2}}$$

where R_G is the radius determined from the Guinier approximation, and $<r>$ is the mean zone radius for the distribution of sizes present. It is, therefore, difficult to detect growth of small zones, which constitute only a small per cent of the total zones, from measurements of the Guinier radius.

In the hardness curve for the Mg-rich alloy, fig. 1, an incubation period precedes the nucleation of the intermediate precipitation, η'. The parameters obtained from X-ray measurements indicate that during this stage a slight zone growth does, however, occur.

For both alloys, a considerable increase in the integrated intensity is observed with time. The integrated intensity can be related to both the volume-fraction of the G-P zones and to the composition of the G-P zones [29]. Therefore, the increase in the value of Q_0, the integrated intensity, in the early stages can be a result of either an increase in the volume-fraction, or due to an increase in the electron density fluctuations between the matrix and the zone due to redistribution of the solute.

Gerold [30] has shown that the type of alloy being studied decomposes homogeneously and that the volume-fraction of the zones remains constant. However, Harkness, Gould, and Hren [31] have recently shown that in some cases, especially in the early stages of ageing, the volume-fraction of the zones may change. It is therefore possible that in the initial period of

ageing, immediately after the quench, the increase in Q_0 is due to the progress of dissociation of the alloy and the formation of the zones. At later stages it is reasonable to assume that the alloy has completely decomposed and that the volume-fraction of the zones remains constant with time. The increase in Q_0 is, at this stage, due only to the increased difference in the electron density of the zone and the matrix. This occurs because of the increasing concentration of the zinc in the zones.

The more rapid increase in the integrated intensity in the Mg-rich alloy is probably due to the fact that segregation is more severe than in the Mg-poor alloy, i.e. the zones in the 1.09 at. % Mg alloy are richer in Zn. This observation is consistent with those found by Ipohorski and Bonfiglioli [18]. These workers assumed that the volume-fraction of the zones does not change, an assumption necessary for the determination of the composition of the zones.

An anomalous increase in the integrated intensity was observed for the Mg-rich alloy at about the same time as the formation of the first intermediate precipitates. The formation of the small η' intermediate precipitate results in streaking, as shown by Belboech and Guinier [32], in a manner similar to the particle size effects in high-angle diffraction. This increase scattering diminishes with the growth of η' precipitate so that Q_0 decreases when the precipitate has grown sufficiently. The scattering at small angles becomes unobservable only when large and incoherent precipitates form.

5. Conclusions

(i) Changes in the zone size follow the same pattern as the changes in hardness so that a close correlation appears to exist between the strength of these alloys and the size of the zones.
(ii) A critical zone size is required for the nucleation of the intermediate precipitate. The critical zone size appears to be dependent on the alloy composition. In the present study it was found to be approximately 43 Å for the 0.72 at. % Mg alloy and approximately 33 Å for the 1.09 at. % Mg alloy.
(iii) The role of Mg as a reversible-vacancy trap has been established. It has also been shown that Mg governs the concentration of Zn in the zones.
(iv) Higher Mg content induces a greater extent of quench clustering, resulting in a large as-quenched hardness difference in alloys having only slightly different Mg contents.

Acknowledgements

We gratefully acknowledge our many helpful discussions with Professor R. W. Gould. We are also indebted to Dr R. W. Hendricks for the use of his laboratory for the SAS measurements and his computer program in analysing our data. This research was supported by an Institutional Grant from the National Aeronautics and Space Administration.

References

1. I. J. POLMEAR, *J. Inst. Metals* **86** (1957-58) 113.
2. *Idem, ibid* **87** (1958-59) 24.
3. *Idem, J. Aust. Inst. Met.* **11** (1966) 246.
4. G. W. LORIMER and R. B. NICHOLSON, *Acta Met.* **14** (1966) 1109.
5. R. B. NICHOLSON, G. THOMAS, and J. NUTTING, *J. Inst. Metals* **87** (1958-59) 429.
6. *Idem, Acta Met.* **8** (1960) 172.
7. J. D. EMBURY and R. B. NICHOLSON, *ibid* **13** (1965) 403.
8. G. THOMAS, and J. NUTTING *J. Inst. Metals* **88** (1959-60) 81.
9. Y. MURAKAMI, S. KOMATSU, and K. NAGATA, *Men. Fac. Eng.*, Kyoto U., XXIX part 2 (1967) 161.
10. C. PANSERI and T. FEDERIGHI, *Acta Met.* **8** (1960) 217.
11. *Idem, ibid* **11** (1964) 575.
12. G. BARTSCH, *ibid* **12** (1964) 270.
13. V. GEROLD and R. W. GOULD, *ibid* p. 954.
14. R. GRAF, *Compt. rend.* **242** (1956) 1311.
15. *Idem, ibid* **244** (1957) 337.
16. A. GUINIER, "Solid State Physics", Vol. 9 (Academic Press, New York, 1959).
17. R. W. GOULD and E. A. STARKE JR, "Advances in X-ray Analysis", Vol. 9 (Plenum Press, New York, 1966) p. 59.
18. M. IPOHORSKI and A. BONFIGLIOLI, *J. Materials Sci.* **2** (1967) 371.
19. L. F. MONDOLFO, N. A. GJOSTEIN, and D. W. LEVINSON, *J. Metals* **8** (1956) 378.
20. H. A. HOLL, *J. Inst. Metals* **93** (1964-65) 364.
21. O. KRATKY, I. PILZ, and P. J. SCHMITZ, *J. Colloid and Interface Sci.* **21** (1966) 24.
22. E. A. STARKE JR, and E. U. LEE, *Matl. Res. Bull.* **2** (1967) 231.
23. A. GUINIER and G. FOURNET, "Small Angle Scattering of X-rays" (Wiley, New York, 1955).
24. E. R. PARKER and T. H. HAZLETT, in "Relation of Properties to Microstructure" (Amer. Soc. Metals, Cleveland, 1954).
25. V. GEROLD and H. SCHMALZRIED, *Z. Metalk.* **49** (1958) 291.
26. V. GEROLD and H. HABERKORN, *ibid* **50** (1959) 568.
27. A. J. PERRY, *Acta Met.* **14** (1966) 1143.

28. R. BAUR and V. GEROLD, *ibid* **12** (1964) 1444.
29. A. GUINIER, "X-ray Diffraction" (Freeman, London, 1963).
30. V. GEROLD, *Phys. Status Solidi* **1** (1961) 37.
31. S. D. HARKNESS, R. W. GOULD, and J. J. HREN, to be published.
32. B. BELBOECH and A. GUINIER, *Acta Met.* **3** (1955) 370.